

GENE REGULATORY NETWORK INFERENCE IN THE PRESENCE OF SELECTION BIAS AND LATENT CONFOUNDERS

Gongxu Luo¹, Haoyue Dai², Boyang Sun¹, Loka Li¹, Biwei Huang³, Petar Stojanov⁴,
Kun Zhang^{1,2}

¹ Mohamed bin Zayed University of Artificial Intelligence

² Carnegie Mellon University

³ University of California San Diego

⁴ Broad Institute of MIT and Harvard

ABSTRACT

Gene Regulatory Network Inference (GRNI) aims to identify causal relationships among genes using gene expression data, providing insights into regulatory mechanisms. A significant yet often overlooked challenge is selection bias—a process where only cells meeting specific criteria, such as gene expression thresholds, survive or are observed, distorting the true joint distribution of genes and thus biasing GRNI results. Furthermore, gene expression is influenced by latent confounders, such as non-coding RNAs, which add complexity to GRNI. To address these challenges, we propose GISL (Gene Regulatory Network Inference in the presence of Selection bias and Latent confounders), a novel algorithm to infer true regulatory relationships in the presence of selection and confounding issues. Leveraging data obtained via multiple gene perturbation experiments, we show that the true regulatory relationships, as well as selection processes and latent confounders can be partially identified without strong parametric models and under mild graphical assumptions. Experimental results on both synthetic and real-world single-cell gene expression datasets demonstrate the superiority of GISL over existing methods.

1 INTRODUCTION

Gene Regulatory Networks (GRNs), where nodes represent genes and directed edges signify cross-gene causal relationships (Levine & Davidson, 2005), play a pivotal role in understanding biological processes at the molecular level and in elucidating the mechanisms of diseases such as cancer (Hanahan & Weinberg, 2000). Gene Regulatory Network Inference (GRNI) refers to the process of reconstructing GRNs from experimental data. In the past decade, the widespread adoption of single-cell RNA sequencing (scRNA-seq) Saliba et al. (2014) and CRISPR-based gene editing technologies Doudna & Charpentier (2014); Larson et al. (2013); Cheng et al. (2013) has enabled the acquisition of vast amounts of single-cell and perturbation data Peidli et al. (2022); Liu et al. (2024), thereby facilitating comprehensive studies of cancer Zhang et al. (2021) and genetic atlases Schaum et al. (2018); Consortium* et al. (2022) at the individual cell level. Causal discovery techniques for GRNI have also been steadily developed to leverage these advances Wang et al. (2017); Belyaeva et al. (2021); Chevalley et al. (2022); Zhang et al. (2023).

Distinguishing true causal relationships between genes from statistical dependencies is a critical challenge in GRNI. Specifically, in the context of scRNA-seq datasets, when two genes exhibit expression dependencies and are conditionally dependent given all subsets of other genes, the question arises whether this implies a direct causal relationship between them. Several existing studies have answered this question with a definitive ‘no’, suggesting that such dependencies may arise from confounding factors, such as hidden confounders like non-coding RNAs and environmental stimuli Gasch et al. (2000); Statello et al. (2021); Razin & Gavrillov (2021). While these studies provide valuable solutions by accounting for confounding influences, we find that even when confounding factors are properly assumed and adjusted for, they cannot fully explain all the observed dependencies in the data. This discrepancy points to the possibility that other unrecognized factors or more complex

causal structures may be at play, necessitating more refined approaches to causal discovery in gene regulation.

To illustrate why hidden confounding alone cannot account for all dependencies, we present a real-data example. Consider two genes, TP73 and CENPF in the Norman dataset (lung carcinoma cell) Thomas M. et al. (2019), for which no direct or indirect causal relationship has been recorded in comprehensive libraries curated by Enrichr Kuleshov et al. (2016). However, as shown in the scatterplot, these genes exhibit a strong and consistent dependency across the dataset. This raises the question: Can confounding factors explain this dependency? To explore this, we analyze perturbation data, which offers a more nuanced insight. In the perturbation data, we observe a significant shift in the marginal distribution of CENPF when TP73 is perturbed, as illustrated in Figure 1. This result contradicts the hypothesis that the observed dependence is due to confounding factors, as perturbing TP73 should not directly affect any confounding factors. While randomized controlled trials (RCTs) are always regarded as the gold standard for causality, no causal link between the two genes can be supported by prior biological knowledge. Thus, we argue that the differential expression observed under perturbation here reflects neither true regulatory relationships nor confounding factors. Instead, it is a result of selection bias.

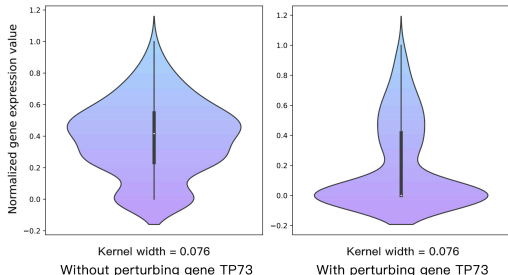


Figure 1: After perturbing gene *TP73*, the distribution of gene *CENPF* change a lot. However, ground truth collected from comprehensive libraries shows they are independent.

Selection refers to a process in which certain elements, individuals, or entities are chosen based on particular criteria or characteristics, and others are excluded. More broadly, in economics, selection is often considered as a process where individuals or entities are chosen based on certain criteria that lead to favorable outcomes, such as higher productivity or profitability. This principle is commonly observed in competitive markets, where only the most efficient businesses survive Aghion (1998). Specifically, in gene expression, selection refers to the “survival of the fittest” at the molecular level, where cells with genes that meet certain constraints are able to survive. For example, genes TP73 and CENPF may not directly regulate each other, yet under specific environmental constraints, they “survive” by adapting to these conditions Alon (2019); Barabási et al. (2011). Returning to the example, if we perturb gene TP73, the observed change in the distribution of gene CENPF may be due to selection.

With this motivation, we develop a causal model that integrates both single-cell observational and perturbation data, using conditional independence (CI) tests to capture dependencies. Our analysis reveals that causal relationships, hidden confounders (a.k.a latent confounders in causal language), and selection processes (the mechanism of selection) exhibit distinct CI patterns. Based on these findings, we propose a novel algorithm, called Gene Regulatory Network Infereⁿce in the presence of Selection bias and Latent confounders (GISL), which aims to identify selection processes as well as causal relationships and hidden confounders.

Contributions. **1.** We are the first, to the best of our knowledge, to identify and to address the issue of selection bias in gene expression data and its impact on GRNI. **2.** We propose a novel algorithm for identifying causal relationships, as well as the presence of latent confounders and selection processes. **3.** Theoretically, the findings of our algorithm are partially identifiable without parametric assumptions under mild graphical conditions. **4.** We validate our claims and demonstrate the effectiveness of our proposed Gene Regulatory Network Inference in the presence of Selection bias and Latent confounders (GISL) on both synthetic and real-world experimental single-cell gene expression data, showing its superiority over canonical causal discovery methods and computational GRNI baselines.

2 PRELIMINARIES AND MOTIVATION

2.1 PRELIMINARIES

A Gene Regulatory Network (GRN) (Levine & Davidson, 2005), which focuses on the causal relations and governing gene activities in cell populations, can be represented by a causal model (Ram et al., 2006). Let the Directed Acyclic Graph (DAG) \mathcal{G} on the vertices $[N] := \{1, \dots, N\}$ represent a causal model, where the vertices correspond to random variables $\mathcal{X} = (X_i)_{i=1}^N$, where each X_i indicates an individual gene. To represent complex cell environments in causal language, the latent confounder $\mathcal{L} = \{L_1, L_2, \dots, L_K\}$ and the selection variable $\mathcal{S} = \{S_1, S_2, \dots, S_K\}$ are involved in \mathcal{G} . $S = \{0, 1\}$ indicates the presence of selection process or not. We can only access the data for which the selection criterion is met, that is, $S_k = 1$. With the available gene expression and perturbation data, *perturbation indicators* $\mathcal{I} = \{I_1, I_2, \dots, I_K\}$ are introduced, each pointing to the corresponding target X_k . $I_k = 0$ denotes observational gene expression data (D_o), $I_k = 1$ represents gene expression data (D_k) after perturbing gene X_k . Variable set $\mathcal{V} = \{\mathcal{X}, \mathcal{L}, \mathcal{S}, \mathcal{I}\}$.

To introduce the different structures of a causal model, the definition of basic terms should be clear.

A causal relation is represented by a directed edge, e.g., $X_i \rightarrow X_j$, where $X_i, X_j \in \mathcal{X}$. This is also described as X_i is the parent of X_j in graph theory. In biology, gene regulation is achieved through an intermediate medium, such as a protein. We also refer to the mechanism underlying a causal relationship as a causal process. If there is a direct path from X_i to X_j , i.e., $X_i \rightarrow \dots \rightarrow X_j$, X_i is called the ancestor of X_j . A latent confounder $L_k \in \mathcal{L}$ acts on a confounded pair in 2.2, forming a hidden common cause ($X_i \leftarrow L_k \rightarrow X_j$), which contributes to dependence that is not causal in nature. The selection process operates on a selection pair 2.3, forming a v-structure ($X_i \rightarrow S_k \leftarrow X_j$) on the selection variable $S_k \in \mathcal{S}$.

As S_k is always given, the joint distribution is $P(\mathcal{X}|S_k)$, resulting in a spurious dependence between X_i and X_j . More basic concepts can be found in A.

$$\begin{aligned} mut(\mathcal{G}, \emptyset) : X &\rightarrow Y \rightarrow Z \\ mut(\mathcal{G}, \{Y\}) : X &\quad Y \rightarrow Z \end{aligned}$$

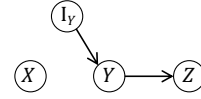
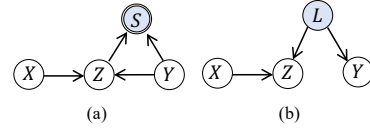


Figure 2: Toy example of hard intervention and corresponding structure.

For hard interventions, Hauser & Bühlmann (2012) consider each I_k as factoring in a mutilated DAG over $[N]$, denoted by $mut(\mathcal{G}, X_k)$, where the edges incoming to the target X_k are removed and others remain as shown in Figure 2. For soft interventions, the mutilated DAG representation fails, as interventions may not remove incoming edges, and all settings may factor in the same \mathcal{G} . When intervening on a cause changes the marginal $p(\text{cause})$ and $p(\text{effect})$, but the conditional $p(\text{effect}|\text{cause})$ remains invariant. Conversely, intervening on an effect leaves $p(\text{cause})$ unchanged, while $p(\text{cause}|\text{effect})$ changes Hoover (1990); Tian & Pearl (2013).



Definition 2.1 (Selection bias) The distribution \mathcal{P} of $X \in \mathcal{X}$ is biased by the selection processes.

Definition 2.2 (Confounded pair) A pair (X_i, X_j) is referred to as a confounded pair, denoted $(X_i, X_j)_l$. If there exist a latent confounders $L_k \in \mathcal{L}$ such that $(X_i \leftarrow L_k \rightarrow X_j)$.

Definition 2.3 (Selection pair) A pair (X_i, X_j) is a selection pair, denoted $(X_i, X_j)_s$, if it follows the structure $(X_i \rightarrow S_k \leftarrow X_j)$, $S_k \subset \mathcal{S}$.

Definition 2.4 (DAG-inducing path (Zhang, 2008)) In a DAG G , if a path p between any two observed vertices (X_i, X_j) relative L, S is called a DAG-inducing path, if it satisfies the following criteria: 1. There is at least one collider on the path p in addition to (X_i, X_j) . 2. Every non-endpoint vertex on p is in L or a collider, and every collider is an ancestor of X_i, X_j , or a member of S . Toy examples are shown in 3.

Assumption 2.5 (Markov) Given a DAG \mathcal{G} and distribution \mathcal{P} over the variable set \mathcal{V} , every variable M in \mathcal{V} is probabilistically independent of its non-descendants given its parents in \mathcal{G} .

Assumption 2.6 (Faithfulness Spirtes et al. (2000)) Given a DAG \mathcal{G} and distribution \mathcal{P} over the variable set \mathcal{V} , \mathcal{P} implies no CI relations not already entailed by the Markov assumption.

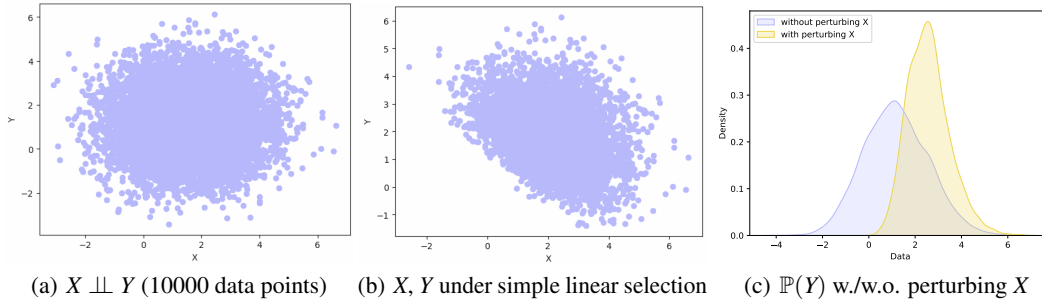


Figure 4: A toy example to introduce (a & b) the selection process, and (c) how it leads to changes in distribution after perturbation despite the absence of the causal relation.

2.2 MOTIVATION

We have introduced the structure of selection processes, let us begin with a toy example to explore the properties of selection. The example shown in Figure 4 illustrates the selection process and how it leads to changes in distribution despite the absence of a causal relationship. We assume that variable X and Y are independent and follow a normal distribution. The causal structure is $X \rightarrow S \leftarrow Y$ (v -structure), where the selection variable S is always given. When applying a simple selection function (e.g. $1.5X + 1.6Y > 3.2$) on them, we can observe the spurious dependence shown in (b). When after perturbing X , the distribution of Y changes significantly as shown in (c) with the **variations in the sample size** (reduced from 5943 to 2601).

With the preliminaries and these observations, we recognize that with a single distribution, it is usually impossible to distinguish dependence induced by the selection process, causal relationships, or latent confounders. Surprisingly, by integrating gene observational and perturbation data, some interesting findings offer insight into tackling this problem. Specifically, the dependencies arising from causal relationships, selection processes, and latent confounders exhibit differences in symmetry and perturbation effects on distributions, making them distinguishable. **Symmetry:** The causal process is asymmetric. Perturbations introduce changes in distribution that propagate exclusively along the causal direction ($X \rightarrow Y$). In contrast, the selection process on both variables is symmetric: Any perturbation on one variable results in a distributional change on the other ($X \rightarrow S \leftarrow Y$). Similarly, the hidden common cause ($X \leftarrow L \rightarrow Y$) is also symmetric, however, the changes in distribution due to perturbation cannot propagate via it, where L is a latent confounder. **Perturbation effects:** In cases of mixed dependencies such as the coexistence of causal relationships with selection processes or latent confounders, symmetry alone is insufficient as a distinguishing criterion. Interestingly, with additional differences in structures, distinct Conditional Independence (CI) patterns emerge between the perturbation indicator (I) and the observed variables as shown in Figure 10 in the Appendix B, offering opportunities to distinguish them.

3 METHODOLOGY

In this section, we construct a causal model to integrate gene observational and perturbation data and propose algorithms for Gene Regulatory Network Inference (GRNI) from a causal perspective. Then, the performance of these algorithms under different structural conditions is discussed.

3.1 GRNI WITHOUT LATENT CONFOUNDERS

By constructing a causal model involving perturbation indicators \mathcal{I} , the gene observational ($I_k = 0$) and perturbation ($I_k = 1$) data are curated. We develop Algorithm 1 (detailed procedure 3), named Gene regulatory network Inference in the presence of Selection Bias (GISB), to discover regulatory relationships (causal structure) among genes and identify selection bias.

GISB and Discussion. Usually without extra information, it is difficult to identify the causal and selection process in the nonparametric setting without graphical conditions. Both causal and selection processes can induce dependence. Thanks to the gene perturbation data, the differences

Algorithm 1 GISB: Gene Regulatory Network Inference in the presence of Selection Bias.

Input: observational data D_o , single gene perturbation data D_i for gene X_i , corresponding perturbation indicators $I_i \subset \mathcal{I}$.

Output: DAG $\mathcal{G} = \{\mathcal{X}, \mathcal{E}\}$, Selection Pairs \mathcal{S} .

- 1: (*Graph Initialization*) Initialize \mathcal{G} as a fully undirected graph and list \mathcal{S} as empty.
 - 2: (*Recovery of skeleton over observational data*) Run skeleton discovery methods on D_o . Remove edges between any pair of vertices if conditional independent or independent. Update \mathcal{G} .
 - 3: (*Recovery of the regulation and selection processes over observational and perturbation data*) For each undirected edge of gene pair (X, Y) in \mathcal{G} , test the marginal and conditional independence between I of one gene and another gene on augmented data $D_{aug} (D_o + D_i)$. Update \mathcal{G} and update \mathcal{S} with identified pairs $(X, Y)_s$.
 - 4: (*Correct spurious relations*) Repeat Step 3 with conditioning on the subsets of non-endpoints on the paths between X and Y in \mathcal{G}_{aug} . Update \mathcal{G} and update \mathcal{S} following the updating rules.
-

between the causal and selection processes emerge, making them distinguishable. With the causal model on perturbation and observational data, an example in Figure 5 shows differences in symmetry, perturbation effects, and structure characters among different structures, which is reflected in CI patterns between \mathcal{I} and observed genes. More details are shown in lines 1, 3, and 5 in Figure 10. The details of Algorithm 1 are as follows: Step 1 initializes a fully connected graph \mathcal{G} . Step 2 deletes independent and conditional independent edges for skeleton discovery, which significantly improves the efficacy of GISB by reducing the size of condition sets. For example, there are two paths between X and Y , $X \rightarrow N \rightarrow Y$ and $X \rightarrow M \leftarrow Y$. $X \perp\!\!\!\perp Y$ can be identified by conditioning on N . The edge between X and Y is removed. Then, dependencies (skeleton) can be explained by causal process, selection process, or combinations. Considering the efficacy of the CI test on high-dimensional gene data, skeleton discovery is not limited to traditional PC. Parallel PC Le et al. (2016) and FGES Ramsey et al. (2017) can be applied. We allow more dependencies, including spurious ones, during skeleton discovery, as these will be further corrected in Step 4. Step 3 collects the results of the CI test with an empty condition set of perturbation indicators \mathcal{I} and a pair of genes. \mathcal{G} and the selection set \mathcal{S} are updated following the rules (the correspondence between the CI patterns and structures) shown in Figure 10. Considering multiple paths, some results in Step 3 need further correcting. For example, the results of (a)-3 and (b)-3 in Figure 12 are the latent confounder with cause and the selection with cause separately. Conditioned on Z , the real structure (X causes Y , X , and Y under selection without cause) is identified. Step 4 further corrects the results of Step 3 by repeating the CI test with traversing subsets of non-endpoint vertices on the path between a pair of perturbed genes as a conditional set. The updating rule is that: when given non-endpoint vertices, if the CI patterns in Step 4 have the same or more dependence, then do not update. If there are fewer dependencies, update \mathcal{G} .

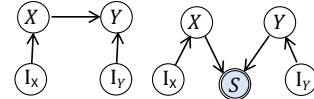


Figure 5: Differences in symmetry and Conditional Independence (CI) patterns: Causation vs. Selection.

3.2 GRNI WITH LATENT CONFOUNDERS

When considering latent confounders, the setting becomes more general, accompanied by a significant increase in the complexity of the graph structure, which also brings greater challenges. Following the same way in building the causal model, we develop Algorithm 2 (detailed procedure 4), named Gene regulatory network Inference in the presence of Selection bias and Latent confounders (GISL). **GISL and Discussion** When considering the general case, which includes latent confounders and selection bias in a nonparametric setting, the graph structure becomes increasingly complex. Similarly to GISB, this approach leverages differences reflected in CI patterns between perturbation indicators \mathcal{I} and observed genes to identify causal structures, selection bias, and latent confounders, including symmetry, perturbation effects, and structural characteristics. The structure of a latent confounder is shown in Figure 6, and detailed structures and CI patterns are in lines 2 and 4 in Figure 10, providing insights into distinguishing them from finding unique markers. Let us start with the algorithm 2 to introduce the interesting laws. Steps 1, 2, and 3 have the same operation

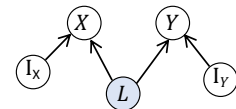


Figure 6: The causal structure of Latent confounders .

Algorithm 2 GISL: Gene Regulatory Network Inferece in the presence of Selection bias and Latent confounders.

Input: observational data D_o , single gene perturbation data D_p for all genes with D_{pi} for gene X_i , perturbation indicator $I_i \subset \mathcal{I}$.

Output: DAG $\mathcal{G} = \{\mathcal{X}, \mathcal{E}\}$, Confounder pairs \mathbf{L} , Selection pairs \mathbf{S} .

- 1: (*Graph Initialization*) Initialize \mathcal{G} as a fully undirected graph and list \mathbf{L} , \mathbf{S} as empty.
 - 2: (*Recovery of regulation skeleton over observational data*) Same as Step 2 in Algorithm 1
 - 3: (*Recovery of the regulation, selection processes, and latent confounders from observational and perturbation data*) Do Step 3 in Algorithm 1. Update \mathcal{G} , \mathbf{L} , \mathbf{S} with identified pairs and mark pairs that need correcting.
 - 4: (*Correction*) Repeat Step 3 with conditioning on the subsets of non-endpoints on the paths between vertex pairs that need correcting in \mathcal{G}_{aug} . Further correct those undetermined pairs following the correction rules, and update \mathcal{G} , \mathbf{L} , \mathbf{S} .
-

as GISB. In Step 3, CI results involving latent with cause, selection with cause, and undetermined ones (all results of the CI test are dependent) will be marked as pairs requiring correction. This is because the skeleton comes from causation, latent confounders, and selection bias. When they meet d-separated paths like $X \rightarrow Z \rightarrow Y$ (chain) or $X \leftarrow Z \rightarrow Y$ (common cause), as the d-separated paths are covered by strong dependencies engendered by causation, latent confounders, and selection bias, they cannot be removed in skeleton discover (Step 2). This results in the wrong CI patterns, as we discussed in Step 3 of GISB. The correcting rules in Step 4 are the same as in GISB: if the CI pattern changes to fewer dependencies in Figure 10, then update \mathcal{G} with new results. If there are the same or more dependencies, do not update. The d-separated paths in Step 3 can be corrected by conditioning on the subsets of non-endpoint vertex between a pair of variables. This is why if there are fewer dependencies, we update them. However, when given some variables like collider, it results in more dependencies, which are spurious ones, so we do not update. For example, lines 2 and 3 in Figure10 will become an all-dependent pattern if colliders are given.

4 IDENTIFIABILITY

4.1 IDENTIFIABILITY WITHOUT LATENT CONFOUNDERS

Is the structure identifiable when selection coexists with other dependencies as shown in Figure 12? To answer this, we establish the identifiability analysis for GISB in the causal and selection process.

Theorem 4.1 (*Identifiability of GISB*) *Let the observational and perturbation data be generated by the DAG model \mathcal{G} defined in Section 2. Suppose that the following conditions hold:*

- *Markov 2.5 and faithfulness 2.6 assumptions.*
- *No latent confounders: $\mathcal{L} = \emptyset$.*

Then, when the sample size $n \rightarrow \infty$, the output DAG \mathcal{G} (qualitative structure information) and the presence of the selection process between gene pairs (under selection bias or not) are identifiable.

Remarks Without latent confounders, the causal process represented by DAG \mathcal{G} is uniquely identified. Intuitively, this is because selection processes do not hinder the identification of causal processes at the level of CI patterns, although the symmetry of selection obscures the underlying asymmetry. Moreover, without latent confounders, DAG-inducing paths cannot produce the same CI patterns as the causal process. Latent confounders are essential to form both arrowheads in causal processes and v-structures necessary to maintain d-connection like (b) in Figure11. The selection structure cannot be uniquely identified. Because DAG-inducing paths can distort CI patterns, e.g., (a)-9 ($X \rightarrow Y \leftarrow I_Y$) and (b)-8 ($X \rightarrow Z \leftarrow Y$) in Figure 12. Because the collider Y and Z is under selection, I_Y and X in (a)-9, X and Y in (b)-8 will always be dependent. It results in the same CI pattern as the selection process. Thus, the selection structures cannot be uniquely determined as we cannot make sure that the selection process directly works on the selection pair (true structure) or vertices in the selection pair and its descendants (DAG-inducing path). Fortunately, both are under selection bias. So, selection bias is identifiable. The comprehensive proof of GISB is in Appendix F.2.

4.2 IDENTIFIABILITY WITH LATENT CONFOUNDERS

We previously discussed methods to identify direct causal relationships and selection mechanisms between genes, assuming no latent confounders. However, in practical scenarios using scRNA-seq data, latent confounders, such as non-gene regulators, transcription factors, and technical covariates, can indeed exist. This raises the question: What can be definitively identified about causal relationships when latent confounders are present?

Theorem 4.2 (*Partial identifiability of GISB*) *Let the observational and perturbation data be generated by the DAG model \mathcal{G} defined in Section 2. Suppose the following conditions hold:*

- *Markov 2.5 and faithfulness 2.6 assumptions.*
- *Selection processes cannot act on latent confounders, that is, latent confounders are not the ancestor of selection variables.*

Then, when the sample size $n \rightarrow \infty$, the qualitative structure information, selection process, and latent confounders are limited to the true structure or the DAG-inducing paths.

Remarks A most generalized model might include latent confounders, perturbation indicators, and observed variables involved in the selection process. Nonetheless, such generalized assumptions often render causal relationships too indeterminate, making the results less informative. For example, a direct causal edge $X \rightarrow Y$ can generally always be replaced with $X \rightarrow S \leftarrow L \rightarrow Y$, where X, Y are observed, L is latent, and S is a selection variable, rendering them indistinguishable in terms of all conditional independence constraints, even with interventional data for I_X and I_Y on both sides.

To address this, we have to adopt a structural assumption: Selection processes involve only observed variables, disallowing any causal edges from latent confounders (\mathcal{L}) and perturbation indicators (\mathcal{I}) to the selection variables \mathcal{S} . This assumption is partly justified by the typically lower prevalence of confounders compared to the variables observed in scRNA-seq data. In this framework, what can we identify? We first notice that even without selection and with interventional data, latent confounders can still make the direct causal relations unidentifiable. Consider the case $X \rightarrow Z \rightarrow Y$ with a latent confounder L_k pointing to both Z and Y shown in Figure 11 (b). Adding a direct edge $X \rightarrow Y$ renders the scenarios equivalent, even if perturbation data I_X, I_Y are available, as the dependence between X and Y cannot solely be explained by Z . With the selection process, in the model $S_1 \leftarrow X \leftarrow L_k \rightarrow Y \rightarrow S_2$ (Figure 11 (a)), whether or not to add a direct edge $X \rightarrow Y$, the two scenarios are unidentifiable. The causal process is identified as limited to ancestor relationships or DAG-inducing paths.

After understanding the DAG-inducing paths, these paths (which are always d-connected) can mimic any structure reflected in conditional independence (CI) patterns. Consequently, the identifiability of latent confounders and the selection process remain constrained by the true structure or the DAG-inducing path. The details of the proof can be found in the Appendix F.2.

5 EXPERIMENTS

In this section, we conduct experiments on synthetic and real-world data sets to validate the claim of the selection process and verify the effectiveness of our proposed GISL in identifying qualitative structure information, selection processes, and latent confounders, demonstrating that it is not only theoretically sound but also leads to superior performance in practice.

5.1 SYNTHETIC DATASETS

Parametric setting. We use a simple structure (X cause Y under selection bias) as an illustrative example to elucidate the setting of the parametric model. The synthetic data is generated according to the structure equation model (SEM) as follows:

$$X = E_x, Y = f(X) + E_y, f_s(X) + f_s(Y) + E_s > 0. \quad (1)$$

where the additive noises, i.e., E_x, E_y as well as E_s are assumed to follow Gaussian distribution with randomly selected means and variances. The causal functions f and selection functions f_s

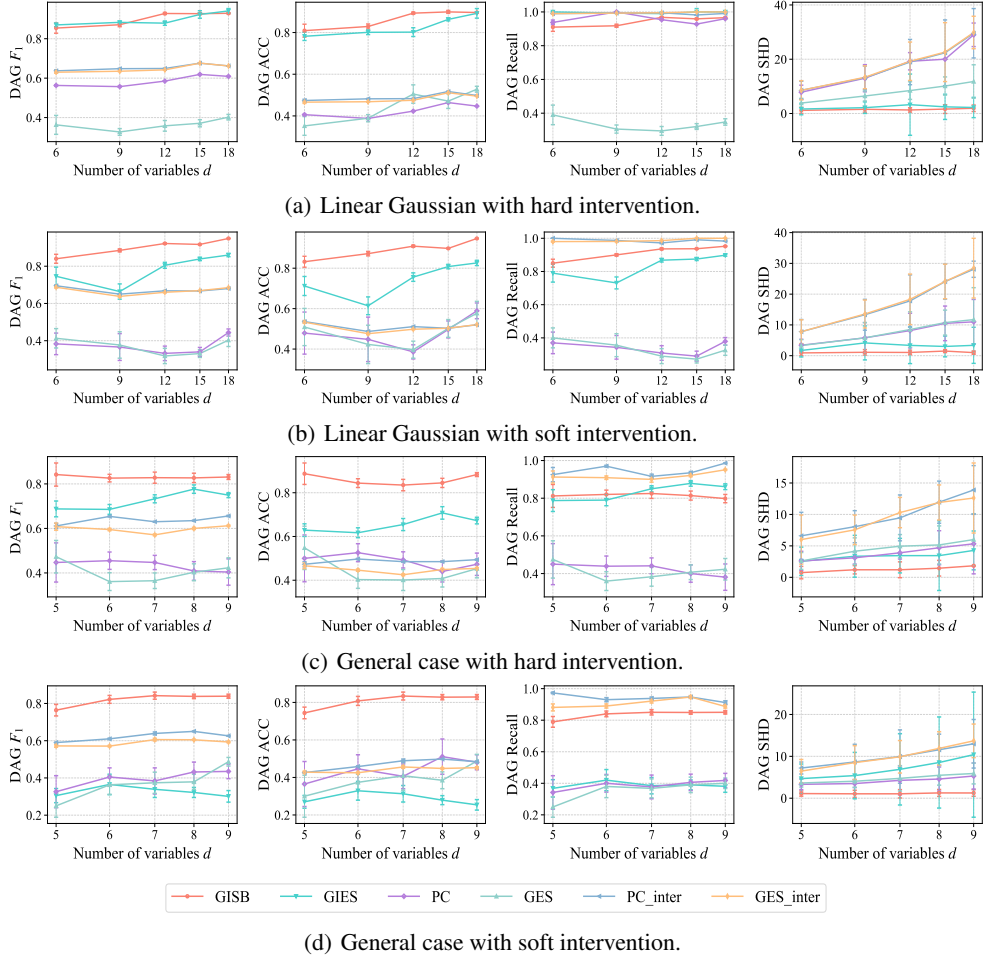


Figure 7: Experimental results of GISL and strong canonical causal discovery baselines on synthetic data sets, where *PC_inter* and *GES_inter* indicate that the results are further refined with perturbation data. By rows, we evaluate different variables d . By columns, we evaluate DAG F_1 (\uparrow), DAG ACC (\uparrow), DAG Recall (\uparrow) and DAG SHD (\downarrow).

are linear with randomly chosen parameters. Gene knockout (CRISPR-Case9) and gene knock-up (CRISPRa) technologies are simulated as hard and soft interventions. The hard intervention sets the gene expression value to 0, while the soft intervention increases the expression value by adding a uniformly distributed noise. Ground-truth causal structures are generated using the Erdős–Rényi model (Erdős et al., 1960) with $d \in \{6, 9, 12, 15, 18\}$ nodes and randomly add 1-3 selection pairs on each causal structure. When considering latent confounders, 1-3 confounder pairs are randomly added. We randomly sample 20 causal structures for experiments.

Nonparametric setting. Unlike a parametric setting, the nonparametric approach accommodates complex nonlinear causal processes. Genes follow the Gaussian distribution with randomly selected means and variances, the causal and selection functions are randomly chosen from linear, square, sin, and tanh functions. To balance complexity and computational efficiency, the ground truth causal structures are generated based on the Erdős–Rényi model with $d \in \{5, 6, 7, 8, 9\}$ nodes, along with 1–2 randomly assigned selection pairs. When latent confounders are considered, 1–2 confounded pairs are randomly included. We randomly sample 20 DAGs for experiments in each setting.

Baselines and evaluation. To evaluate the effectiveness of our proposed GISL, we report the Structural Hamming distance (SHD), F1 score, precision, and recall to measure the quality of predictions against ground truth on synthetic datasets compared with canonical baselines. Without latent confounders, PC (Spirtes & Glymour, 1991), GES (Chickering, 2002), and GIES (Hauser & Bühlmann, 2012) algorithms are used as strong baselines. At the same time, the GISL outputs a

DAG, and the PC, GES, and GIES output a completed partially directed acyclic graph (CPDAG). To ensure consistency at the data level, we use the simple orientation rules (Dor & Tarsi, 1992) implemented by Causal-DAG (Chandler Squires, 2018) to uncover more edges in CPDAG with the help of perturbation data. With latent confounders, the FCI (Spirtes et al., 1995; Zhang, 2008) and ICD (Rohekar et al., 2021) are set as baselines. We report the metrics on PAG compared with baselines. Moreover, computational methods are also discussed in the Appendix G.2.

Table 1: Experimental results on different numbers of selection processes. #S indicates the number of selection process, SACC denotes the accuracy of identifying selection structures.

#S	1	2	3	4	1	2	3	4
	Hard intervention				Soft intervention			
ACC	88.4±1.1	80.5±0.6	73.6±0.6	65.9±1.4	90.4±0.5	85.3±0.9	80.2±0.7	77.5±1.3
Recall	94.4±0.8	93.3±0.6	90.5±1.0	85.8±1.8	93.8±0.5	91.1±0.6	90.0±0.8	88.9±0.5
F1	91.2±0.9	86.4±0.5	81.1±0.7	74.4±1.5	92.1±0.4	88.1±0.7	84.6±0.6	82.6±0.9
SHD	1.2±1.1	2.1±0.7	2.9±1.0	4.1±2.6	0.9±0.4	1.45±0.9	2.1±0.9	2.4±2.0
SACC	60.8±17.8	65.6±8.2	68.4±3.6	45.4±6.4	70.5±1.6	72.1±4.5	56.9.6±7.7	49.5±14.3

Experimental results without latent confounders. We conduct experiments and a comparative analysis on synthetic data sets to validate our claims about GISB in identifying qualitative structure information, and selection process. First, the priority of introducing perturbation data is evaluated on synthetic data without selection bias as shown in Figure 14. Experimental results for GISB and the baseline methods across all evaluation criteria are presented in Figure 7. From Figure 7, we can see that our method shows its superiority over all baselines in different criteria. The reasons are as follows: First, the spurious dependence engendered by selection bias can not be handled by baselines. Second, even with perturbation data, causal processes are still not distinguishable under selection bias. This is because the stronger symmetry property of the selection process covers up the asymmetry of the causal process, leading to the unidentifiable existence of qualitative information. However, instead of directly using changes in distribution, our algorithm models the difference in symmetry and structures of selection and causal processes by introducing a perturbation indicator I as a surrogate variable. The distinction can be expressed through the conditional independence relations between the surrogate variable and the genes. This design cleverly avoids the drawbacks of baselines and identifies the causal structure for GRNI. Moreover, selection bias can be identified. Following the algorithm 1, to start with, we try to distinguish different patterns based on CI test results, but there appear spurious dependencies engendered by selection bias. The reasons are as follows: one is the transitivity of the selection mechanism such as (a)-8 in Figure 12, if the selection process works on the descendants of observed ones, the CI test results show the existence of selection bias. We tackle it by traversing all subsets of nodes on the paths between X and Y . This leads to another case like (a)-6, if the adjacent node forms a v -structure with X and Y is given, there will form the illusion of selection bias. Another is the Y structure with the selection variable S as the descendant of the collider, which will break the conditional independent relations by introducing dependence since S is always given. Although the structure of the selection process is not determined, all are under selection bias due to the presence of the selection process.

To evaluate the effectiveness of our proposed GISB in identifying the presence of selection bias, we conduct experiments on causal graphs with $d=10$ nodes in both linear Gaussian and general cases, considering various numbers of node pairs subject to selection processes. We randomly generate 20 causal structures for each setting. Experimental results on all evaluation criteria are shown in Table 1. With the increasing number of selection processes, GISB still keeps competitive performance even though almost all variables are under selection bias. Due to the partial identifiability of selection bias, the accuracy of identifying selection structures is around 50% to 70%.

Experimental results with latent confounders. Experiments are carried out to validate the ability of GISL to identify qualitative structure information, selection processes, and latent confounders. In Figure 8, experimental results in nonparametric settings show the superiorities over FCI and ICD methods. Moreover, the average accuracy for identifying selection structures is 0.708 ± 0.194 and 0.910 ± 0.005 for soft and hard intervention, separately. The average accuracy for identifying latent confounders is 0.841 ± 0.189 and 0.654 ± 0.186 . The reasons are similar to the case that does not

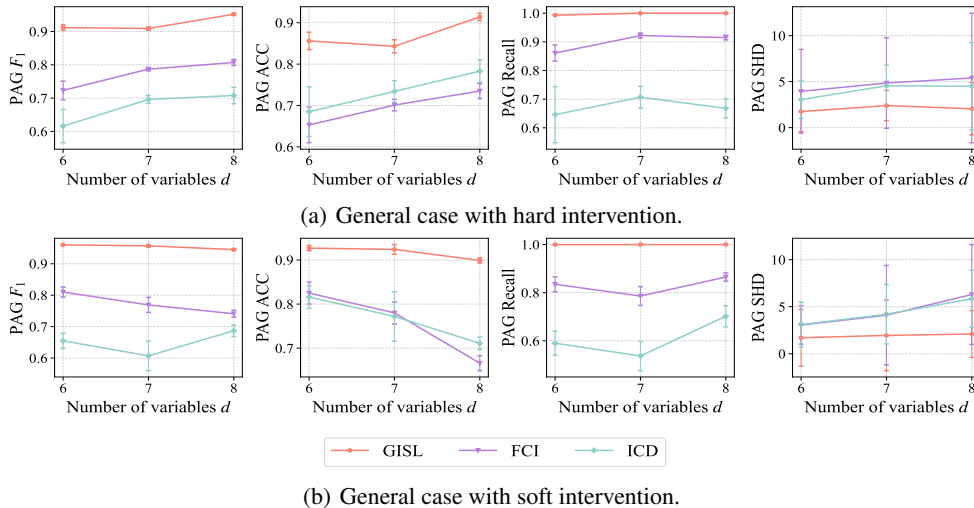


Figure 8: Experimental results on PAG F_1 (\uparrow), PAG ACC (\uparrow), PAG Recall (\uparrow) and PAG SHD (\downarrow).

consider latent confounders. Integrating differences in symmetry and CI patterns, causal processes, selection processes, and latent confounders are distinguishable.

5.2 REAL-WORLD EXPERIMENTAL DATASETS

To examine the efficacy of GISL and validate our claim of the overlooked selection process in a real-world setting, we apply our method to gene expression data collected by Perturb-seq (Thomas M. et al., 2019). Data are collected from lung carcinoma cells (A-549) with 5045 observable genes and 7353 cells. Furthermore, the CRISPRa gene knock-up technique is utilized in cultured cells to enhance the expression value of 105 genes separately, resulting in gene perturbation data. Firstly, GISL discovers the skeleton among 5045 genes, followed by identifying the structure of perturbed gene pairs. We evaluate GISL on perturbed genes, comparing it with prior knowledge provided by Enrichr (Kuleshov et al., 2016; Chen et al., 2013; Xie et al., 2021) which collects comprehensive libraries. In addition, to verify the presence of selection bias, we argue that for each pair of genes, if they are in the presence of selection bias, the number of survived cells varies over perturbing different genes on the premise of culturing the same number of cells. Fortunately, with the CRISPR experimental records organized by DepMap (DepMap, 2023), a cell population dynamics model was proposed for cell proliferation dynamics, where the z-score was designed to show differences in growth rate between normal cells and perturbed ones. The higher value indicates a significant change in the number of surviving cells following gene perturbation (Dempster et al., 2019; 2021; Pacini et al., 2021). A subgraph of genes with perturbation data as shown in Figure 9. The results for all perturbed genes are presented in Figure 18. From the figure, one can see that the GISL introduces numerous edges and selection processes that are backed by prior knowledge. For example, Gene *FEV*, *PTPN1*, and *SET* are under a selection process with z-scores 0.11, -0.204, and -0.167, respectively. The distribution of the z-scores of these genes across all cell lines is shown in Figure 15, providing evidence that selection processes contribute to the observed differential gene expression. Another advantage of our method is that GISL is not limited to perturbing all genes. In experimental conditions, we only perturb genes that we want to discover the relationship instead of perturbing genes without guidance, which is time-saving and source-saving. For experimental details and results on other real-world experimental datasets, please refer to Appendix H.

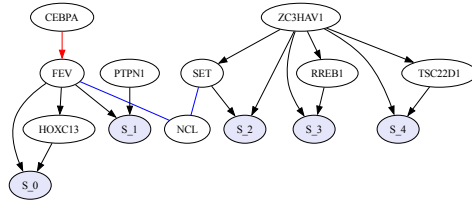


Figure 9: Experimental results on a subset of genes with perturbation data. GISL predicts red edges but mismatches with Enrichr (Chen et al., 2013). Black edges are returned by GISL backed by Enrichr. The blue edges indicate that the structure remains undetermined.

6 CONCLUSION AND DISCUSSION

Rethinking differential gene expression and the observed distributional changes in unregulated genes from gene perturbation data, we argue that the overlooked selection process and the presence of latent confounders significantly bias the performance of gene regulatory network inference (GRNI). Many confusing dependent patterns observed in gene expression data can be explained by the selection inclusion and latent confounders. Although with a single distribution, it is generally difficult to identify the causal process, selection process, and latent confounders, thanks to gene perturbation data, which provide observations of the differences in symmetry and perturbation effect among them, resulting in distinguishable conditional independent patterns. This motivates us to establish a set of theoretical results demonstrating the partial identifiability of qualitative structure information, latent confounders, and selection processes without any parametric and graphical assumptions. At the same time, we propose a novel GISL algorithm to recover the selection process and latent confounders from causal relations in confusing dependencies among genes. The validity of the presence of the selection process, theoretical claims, and the algorithm's efficacy have been rigorously evaluated on synthetic and real-world data. For limitations and discussion, please kindly refer to Appendix I

REFERENCES

- Britt Adamson, Thomas M Norman, Marco Jost, Min Y Cho, James K Nuñez, Yuwen Chen, Jacqueline E Villalta, Luke A Gilbert, Max A Horlbeck, Marco Y Hein, et al. A multiplexed single-cell crispr screening platform enables systematic dissection of the unfolded protein response. *Cell*, 167(7):1867–1882, 2016a.
- Britt Adamson, ThomasM. Norman, Marco Jost, MinY. Cho, JamesK. Nuñez, Yu-Wen Chen, JacquelineE. Villalta, LukeA. Gilbert, MaxA. Horlbeck, MarcoY. Hein, RyanA. Pak, AndrewN. Gray, CarolA. Gross, Oren Parnas, JonathanS. Weissman, Atray Dixit, and Aviv Regev. A multiplexed single-cell crispr screening platform enables systematic dissection of the unfolded protein response. *PMC,PMC*, Nov 2016b.
- Philippe Aghion. Endogenous growth theory. *MIT Press google schola*, 2:155–173, 1998.
- Uri Alon. *An introduction to systems biology: design principles of biological circuits*. Chapman and Hall/CRC, 2019.
- Albert-László Barabási, Natali Gulbahce, and Joseph Loscalzo. Network medicine: a network-based approach to human disease. *Nature reviews genetics*, 12(1):56–68, 2011.
- Anastasiya Belyaeva, Chandler Squires, and Caroline Uhler. Dci: learning causal differences between gene regulatory networks. *Bioinformatics*, 37(18):3067–3069, 2021.
- Thalia E Chan, Michael PH Stumpf, and Ann C Babbitt. Gene regulatory network inference from single-cell data using multivariate information measures. *Cell systems*, 5(3):251–267, 2017.
- Chandler Squires. *causal DAG: creation, manipulation, and learning of causal models*, 2018. URL <https://github.com/uhlerlab/causal DAG>.
- Edward Y Chen, Christopher M Tan, Yan Kou, Qiaonan Duan, Zichen Wang, Gabriela Vaz Meirelles, Neil R Clark, and Avi Ma’ayan. Enrichr: interactive and collaborative html5 gene list enrichment analysis tool. *BMC bioinformatics*, 14(1):1–14, 2013.
- Albert W Cheng, Haoyi Wang, Hui Yang, Linyu Shi, Yarden Katz, Thorold W Theunissen, Sudharshan Rangarajan, Chikdu S Shivalila, Daniel B Dadon, and Rudolf Jaenisch. Multiplexed activation of endogenous genes by crispr-on, an rna-guided transcriptional activator system. *Cell research*, 23(10):1163–1171, 2013.
- Mathieu Chevalley, Yusuf Roohani, Arash Mehrjou, Jure Leskovec, and Patrick Schwab. Causalbench: A large-scale benchmark for network inference from single-cell perturbation data. *arXiv preprint arXiv:2210.17283*, 2022.
- David Maxwell Chickering. Optimal structure identification with greedy search. *Journal of machine learning research*, 3(Nov):507–554, 2002.
- The Tabula Sapiens Consortium*, Robert C Jones, Jim Karkanias, Mark A Krasnow, Angela Oliveira Pisco, Stephen R Quake, Julia Salzman, Nir Yosef, Bryan Bulthaupt, Phillip Brown, et al. The tabula sapiens: A multiple-organ, single-cell transcriptomic atlas of humans. *Science*, 376(6594):eabl4896, 2022.
- Joshua M Dempster, Jordan Rossen, Mariya Kazachkova, Joshua Pan, Guillaume Kugener, David E Root, and Aviad Tsherniak. Extracting biological insights from the project achilles genome-scale crispr screens in cancer cell lines. *BioRxiv*, pp. 720243, 2019.
- Joshua M Dempster, Isabella Boyle, Francisca Vazquez, David Root, Jesse S Boehm, William C Hahn, Aviad Tsherniak, and James M McFarland. Chronos: a crispr cell population dynamics model. *BioRxiv*, pp. 2021–02, 2021.
- DepMap. Depmap 23q4 public. figshare+. *Journal Name*, 2023. URL <https://doi.org/10.25452/figshare.plus.24667905.v2>.
- Atray Dixit, Oren Parnas, Biyu Li, Jenny Chen, CharlesP. Fulco, Livnat Jerby-Arnon, NemanjaD. Marjanovic, Danielle Dionne, Tyler Burks, Raktima Raychowdhury, Britt Adamson, ThomasM. Norman, EricS. Lander, JonathanS. Weissman, Nir Friedman, and Aviv Regev. Perturb-seq: Dissecting molecular circuits with scalable single-cell rna profiling of pooled genetic screens. *PMC,PMC*, Nov 2016.
- Dorit Dor and Michael Tarsi. A simple algorithm to construct a consistent extension of a partially oriented graph. *Technical Report R-185, Cognitive Systems Laboratory, UCLA*, pp. 45, 1992.
- Jennifer A. Doudna and Emmanuelle Charpentier. The new frontier of genome engineering with crispr-cas9. *Science*, Nov 2014. doi: 10.1126/science.1258096. URL <http://dx.doi.org/10.1126/science.1258096>.

- Paul Erdős, Alfréd Rényi, et al. On the evolution of random graphs. *Publ. math. inst. hung. acad. sci.*, 5(1): 17–60, 1960.
- Audrey P Gasch, Paul T Spellman, Camilla M Kao, Orna Carmel-Harel, Michael B Eisen, Gisela Storz, David Botstein, and Patrick O Brown. Genomic expression programs in the response of yeast cells to environmental changes. *Molecular biology of the cell*, 11(12):4241–4257, 2000.
- Douglas Hanahan and Robert A Weinberg. The hallmarks of cancer. *cell*, 100(1):57–70, 2000.
- Alain Hauser and Peter Bühlmann. Characterization and greedy learning of interventional markov equivalence classes of directed acyclic graphs. *The Journal of Machine Learning Research*, 13(1):2409–2464, 2012.
- Kevin D Hoover. The logic of causal inference: Econometrics and the conditional analysis of causation. *Economics & Philosophy*, 6(2):207–234, 1990.
- Alexandra B Keenan, Denis Torre, Alexander Lachmann, Ariel K Leong, Megan L Wojciechowicz, Vivian Utti, Kathleen M Jagodnik, Eryk Kropiwnicki, Zichen Wang, and Avi Ma’ayan. Chea3: transcription factor enrichment analysis by orthogonal omics integration. *Nucleic acids research*, 47(W1):W212–W224, 2019.
- Seongho Kim. ppcor: an r package for a fast calculation to semi-partial correlation coefficients. *Communications for statistical applications and methods*, 22(6):665, 2015.
- Maxim V Kuleshov, Matthew R Jones, Andrew D Rouillard, Nicolas F Fernandez, Qiaonan Duan, Zichen Wang, Simon Koplev, Sherry L Jenkins, Kathleen M Jagodnik, Alexander Lachmann, et al. Enrichr: a comprehensive gene set enrichment analysis web server 2016 update. *Nucleic acids research*, 44(W1):W90–W97, 2016.
- Matthew H Larson, Luke A Gilbert, Xiaowo Wang, Wendell A Lim, Jonathan S Weissman, and Lei S Qi. Crispr interference (crispr) for sequence-specific control of gene expression. *Nature protocols*, 8(11):2180–2196, 2013.
- Thuc Duy Le, Tao Hoang, Jiuyong Li, Lin Liu, Huawen Liu, and Shu Hu. A fast pc algorithm for high dimensional causal discovery with multi-core pcs. *IEEE/ACM transactions on computational biology and bioinformatics*, 16(5):1483–1495, 2016.
- Michael Levine and Eric H Davidson. Gene regulatory networks for development. *Proceedings of the National Academy of Sciences*, 102(14):4936–4942, 2005.
- Qi Liu, Ling Guo, Zhiting Wei, Duanmiao Si, Bin Duan, Yicheng Gao, and Qian Yu. Perturbbase: a comprehensive database for single-cell perturbation data analysis and visualization. *bioRxiv*, pp. 2024–02, 2024.
- Clare Pacini, Joshua M Dempster, Isabella Boyle, Emanuel Gonçalves, Hanna Najgebauer, Emre Karakoc, Dieudonne van der Meer, Andrew Barthorpe, Howard Lightfoot, Patricia Jaaks, et al. Integrated cross-study datasets of genetic dependencies in cancer. *Nature communications*, 12(1):1661, 2021.
- Stefan Peidli, Tessa Durakis Green, Ciyue Shen, Torsten Gross, Joseph Min, Jake Taylor-King, Debora Marks, Augustin Luna, Nils Bluthgen, and Chris Sander. scperturb: Information resource for harmonized single-cell perturbation data. *bioRxiv*, 2022.
- Ramesh Ram, Madhu Chetty, and Trevor I Dix. Causal modeling of gene regulatory network. In *2006 IEEE Symposium on Computational Intelligence and Bioinformatics and Computational Biology*, pp. 1–8. IEEE, 2006.
- Joseph Ramsey, Madelyn Glymour, Ruben Sanchez-Romero, and Clark Glymour. A million variables and more: the fast greedy equivalence search algorithm for learning high-dimensional graphical causal models, with an application to functional magnetic resonance images. *International journal of data science and analytics*, 3: 121–129, 2017.
- Sergey V Razin and Alexey A Gavrilov. Non-coding rnas in chromatin folding and nuclear organization. *Cellular and Molecular Life Sciences*, 78(14):5489–5504, 2021.
- Raanan Y Rohekar, Shami Nisimov, Yaniv Gurwicz, and Gal Novik. Iterative causal discovery in the possible presence of latent confounders and selection bias. *Advances in Neural Information Processing Systems*, 34: 2454–2465, 2021.
- Antoine-Emmanuel Saliba, Alexander J. Westermann, Stanislaw A. Gorski, and Jörg Vogel. Single-cell rna-seq: advances and future challenges. *Nucleic Acids Research*, pp. 8845–8860, Aug 2014. doi: 10.1093/nar/gku555. URL <http://dx.doi.org/10.1093/nar/gku555>.

- Nicholas Schaum, Jim Karkanas, Norma F Neff, Andrew P May, Stephen R Quake, Tony Wyss-Coray, Spyros Darmanis, Joshua Batson, Olga Botvinnik, Michelle B Chen, et al. Single-cell transcriptomics of 20 mouse organs creates a tabula muris: The tabula muris consortium. *Nature*, 562(7727):367, 2018.
- Peter Spirtes and Clark Glymour. An algorithm for fast recovery of sparse causal graphs. *Social science computer review*, 9(1):62–72, 1991.
- Peter Spirtes, Clark N Glymour, Richard Scheines, and David Heckerman. *Causation, prediction, and search*. MIT press, 2000.
- Peter L Spirtes, Christopher Meek, and Thomas S Richardson. Causal inference in the presence of latent variables and selection bias. *Conference on Uncertainty in Artificial Intelligence*, 1995.
- Luisa Statello, Chun-Jie Guo, Ling-Ling Chen, and Maite Huarte. Gene regulation by long non-coding rnas and its biological functions. *Nature reviews Molecular cell biology*, 22(2):96–118, 2021.
- Norman Thomas M., Horlbeck Max A., Replogle Joseph M., Ge Alex Y., Xu Albert, Jost Marco, Gilbert Luke A., and Weissman Jonathan S. Exploring genetic interaction manifolds constructed from rich single-cell phenotypes. *Science*, Nov 2019.
- Jin Tian and Judea Pearl. Causal discovery from changes. *arXiv preprint arXiv:1301.2312*, 2013.
- Yuhao Wang, Liam Solus, Karren Yang, and Caroline Uhler. Permutation-based causal inference algorithms with interventions. *Advances in Neural Information Processing Systems*, 30, 2017.
- Zhuorui Xie, Allison Bailey, Maxim V Kuleshov, Daniel JB Clarke, John E Evangelista, Sherry L Jenkins, Alexander Lachmann, Megan L Wojciechowicz, Eryk Kropiwnicki, Kathleen M Jagodnik, et al. Gene set knowledge discovery with enrichr. *Current protocols*, 1(3):e90, 2021.
- Jiaqi Zhang, Louis Cammarata, Chandler Squires, Themistoklis P Sapsis, and Caroline Uhler. Active learning for optimal intervention design in causal models. *Nature Machine Intelligence*, 5(10):1066–1075, 2023.
- Jiji Zhang. On the completeness of orientation rules for causal discovery in the presence of latent confounders and selection bias. *Artificial Intelligence*, 172(16-17):1873–1896, 2008.
- Yijie Zhang, Dan Wang, Miao Peng, Le Tang, Jiawei Ouyang, Fang Xiong, Can Guo, Yanyan Tang, Yujuan Zhou, Qianjin Liao, et al. Single-cell rna sequencing in cancer research. *Journal of Experimental & Clinical Cancer Research*, 40:1–17, 2021.

Appendix

A CONCEPTS

Definition A.1 (Marginal independence test) Check whether two variables X and Y are independent of each other without considering any other variables. Mathematically: $X \perp\!\!\!\perp Y$, meaning X and Y are independent in the overall data distribution.

Definition A.2 (Conditional independence test) Evaluate whether two variables X and Y are independent given a third variable or set of variables Z . Mathematically: $X \perp\!\!\!\perp Y|Z$, meaning X and Y are independent conditioned on Z .

Definition A.3 (d-separation) If every path from a node in X to a node in Y is d-separated by Z , then X and Y are always conditionally independent given Z .

Definition A.4 (d-connection) If every path from a node in X to a node in Y is d-connected by Z , then X and Y are always conditionally dependent given Z .

Definition A.5 (Partial identifiability) Not all causal structures can be uniquely determined from the available data and assumptions. However, the set of plausible structures can be identified.

Definition A.6 (Identifiability) The causal structures are uniquely determined from the observed data.

B MOTIVATING EXAMPLE OF DISTINGUISHABLE CI PATTERNS

We provide basic examples in Figure 10 to show our insight into distinguishing causal processes, selection processes, and latent confounders based on conditional independence (CI) patterns. The differences in symmetry and structures result in different CI patterns, making them distinguishable. Some cases as shown in Figure 11 are unidentifiable in discovering causal processes, as the causal dependencies engendered by the inducing path shown in the second and third cases can not be distinguished from the real causal process. Moreover, the first case results in latent with cause, where the Y-structure formed by I_X, X, L, S introduces the dependence that can not be d-separated between I_X and L . This dependence leads to spurious CI patterns, posing a challenge for our algorithm in identifying the causal process. The identifiability of GISB and GISL is discussed in F.2

C EXAMPLES TO SHOW THE IDENTIFIABILITY OF GISB

Some examples in Figure 12 show insight into identifying different patterns based on CI patterns in the case without latent confounders. The examples are listed to support the discussion about GISB in Section 3. Specifically, the causal processes are identifiable, the dotted ones show partial identifiability in the structure of selection processes. As inducing path and Y-structure like (b)-8 and (a)-9, this results in the d-connected path leading to the phenomenon that changes in distribution can propagate along this path. Then we cannot identify the selection structure, at the same time, we can identify the presence of selection bias.

D THE PROCEDURE OF ALGORITHM 1

The details of GISB are shown in Algorithm 3. Every step is introduced, including how to utilize the observational and perturbation data.

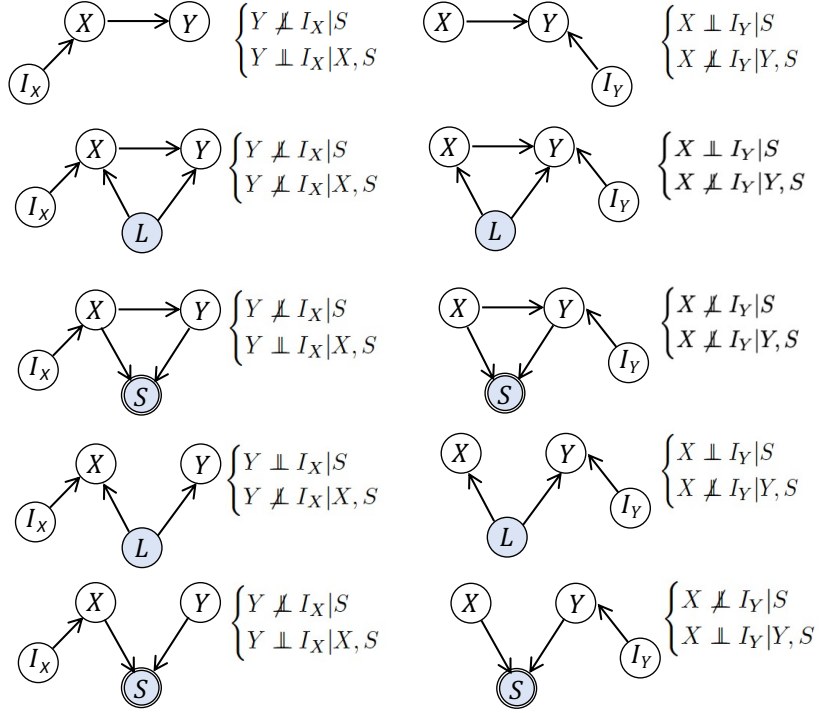


Figure 10: Examples of distinguishable CI patterns, where S is the selection variable indicating the selection process, L is the latent confounder, X and Y are observed variables.

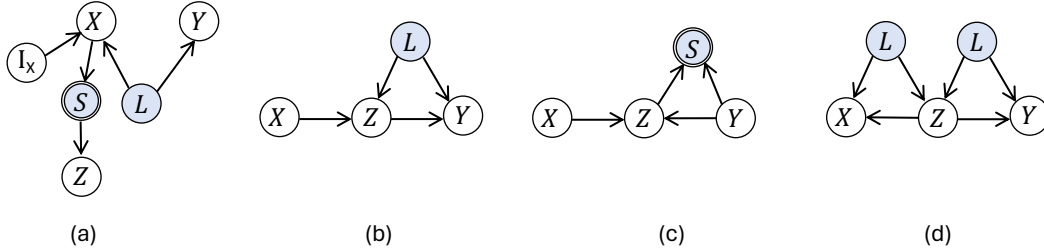


Figure 11: Examples of DAG-inducing path (non-identifiable cases), where X and Y are always d-connected.

E THE PROCEDURE OF ALGORITHM 2

The details of GISL are shown in Algorithm 4. We detail all the steps of the algorithm, similar to how they are listed in GISB.

F PROOF

F.1 THEOREM 3.1

Proof. 1. The unique CI patterns of causal relationships are $X \perp\!\!\!\perp I_Y$ and $Y \not\perp\!\!\!\perp I_X | S$. where $Y \not\perp\!\!\!\perp I_X | S$ needs X and Y to be d-connected and no nodes beside I_X point to X . However, $X \perp\!\!\!\perp I_Y$ can only be satisfied when $X - Y - I_Y$ forms a v-structure, which means that there is an edge point to Y shown in Figure 13 (a). In total, between X and Y , in addition to the causal process, if other paths satisfy the previous requirement, there must exist a v-structure, i.e. $X \rightarrow Z \leftarrow Y$, and Z is given, as there is an edge point to Y , it will form a loop, which conflicts with the DAG assumption. However, the v-structure cannot point to Y conflicts with the necessary conditions. **2.** Identify the

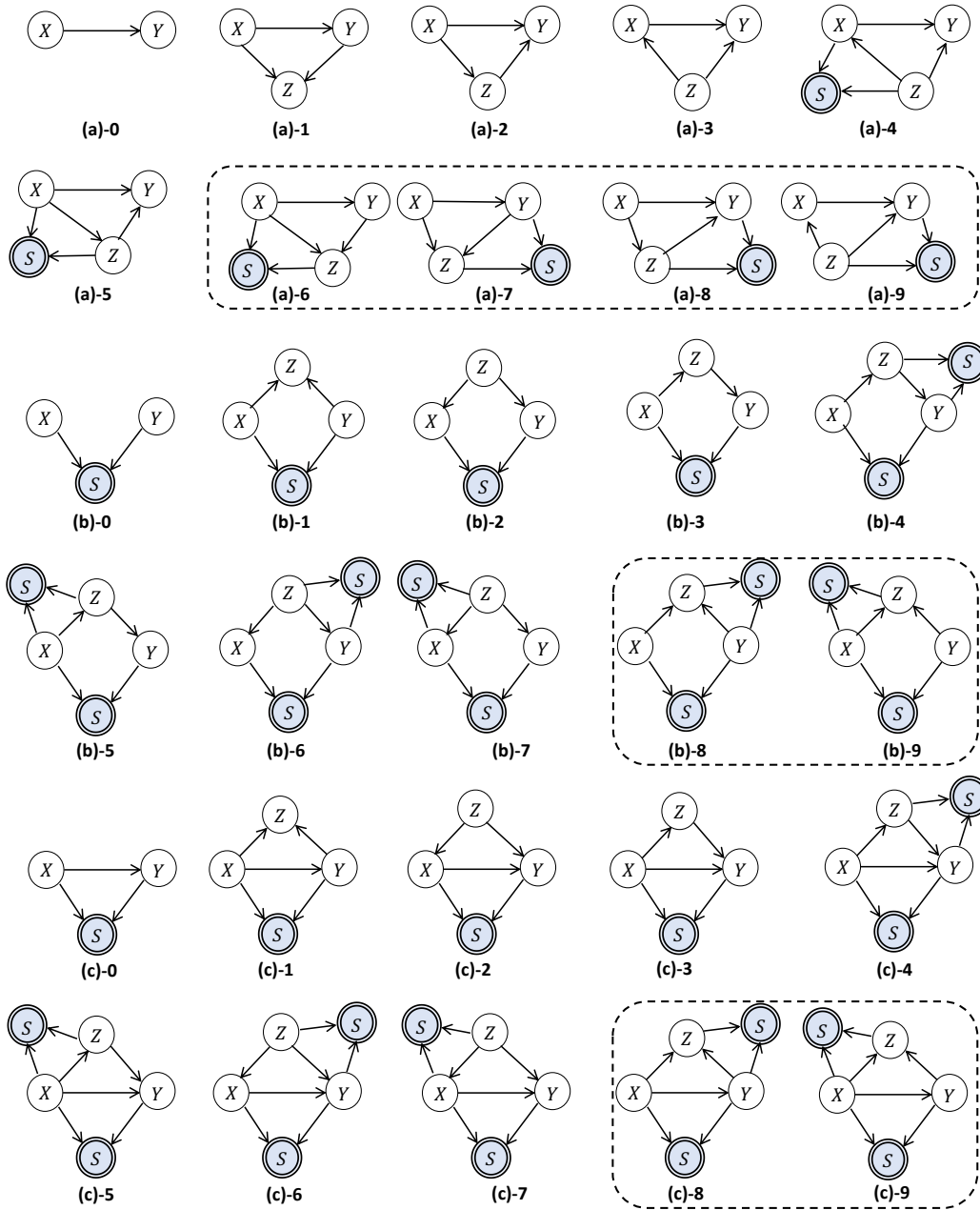


Figure 12: Examples of causal graphs with three observable variables. The graphs in the dotted box share the same conditional independence relations, and all the other graphs outside the dotted box have different conditional independence relations.

selection process. The selection process needs $X \perp\!\!\!\perp I_Y | Y, S$, and $Y \perp\!\!\!\perp I_X | X, S$ as shown in Figure 13 (b). Any paths between X, Y (point to X, Y) apart from the v-structure will conflict with the CI pattern. However, the v-structure is independent given \emptyset , which can be distinguished. **3.** Selection with cause. The required structure is shown in Figure 13 (c). X and I_Y are always conditionally dependent. It forms a unique Y-structure, that is, $X \rightarrow Y \leftarrow I_Y, Y \rightarrow S$. As S is always given, it is mandatory. The proof of the causal process is the same as in the previous part. However, the selection process cannot be determined between X, Y , or the descendant of X and Y . Proof done.

Algorithm 3 Concrete procedure of GISB

Input: observational data D_o , single gene perturbation data D_p for perturbed genes with D_{pi} for gene i .

Output: DAG $\mathcal{G} = (\mathcal{V}, \mathcal{E})$, selection pair \mathcal{S} .

Step 1:

Initialize $\mathcal{G} = (\mathcal{V}, \mathcal{E})$ as fully-connected graph. List \mathcal{S} selection pairs as empty.

Step 2:

All $s \in \mathcal{S}$ is given.

for any pair of genes (x, y) in \mathcal{V} do

if $x \perp\!\!\!\perp y$ | any subset of $\mathcal{V} - \{x, y\}$ on D_o then

remove the edge between x and y from \mathcal{E} , update \mathcal{G} .

end if

end for

Step 3:

Introduce surrogate variable (perturbation indicator) $I = 0$ for D_o and $I = 1$ for D_p .

for edge between genes (x, y) in \mathcal{E} do

Construct D_x by concatenating D_o with $I_X = 0$ and D_{px} with $I_X = 1$. Similarly, construct D_y .

if $x \perp\!\!\!\perp I_Y$ | s on D_y then

x cause y , update \mathcal{G} .

else if $y \perp\!\!\!\perp C_x$ | s on D_x then

y cause x , update \mathcal{G} .

else if $x \not\perp\!\!\!\perp C_y$ | s ; $x \perp\!\!\!\perp C_y$ | y, s on D_y and $y \not\perp\!\!\!\perp C_x$ | s ; $y \perp\!\!\!\perp C_x$ | x, s on D_x then

x and y under selection without cause, update \mathcal{S} with (x, y) .

else

Step 4:

for subsets t of nodes on the paths from x to y do

if $x \perp\!\!\!\perp C_y$ | t, s on D_y then

x cause y , update \mathcal{G} .

else if $y \perp\!\!\!\perp C_x$ | t, s on D_x then

y cause x , update \mathcal{G} .

else if $x \not\perp\!\!\!\perp C_y$ | t, s ; $x \perp\!\!\!\perp C_y$ | t, y, s on D_y and $y \not\perp\!\!\!\perp C_x$ | t, s ; $y \perp\!\!\!\perp C_x$ | t, x, s on D_x then

x and y are under selection without cause, update \mathcal{S} with (x, y) .

else if $x \not\perp\!\!\!\perp C_y$ | t, s and $x \perp\!\!\!\perp C_y$ | t, y, s on D_y then

x cause y under selection, update \mathcal{G} , update \mathcal{S} with (x, y) .

else if $y \not\perp\!\!\!\perp C_x$ | t, s and $y \perp\!\!\!\perp C_x$ | t, x, s on D_x then

y cause x under selection, update \mathcal{G} , update \mathcal{S} with (x, y) .

end if

end for

end if

return DAG $\mathcal{G} = (\mathcal{V}, \mathcal{E})$, selection pairs \mathcal{S} .

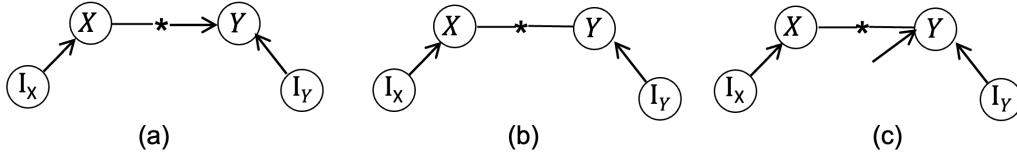


Figure 13: Required structure for causal relation, latent confounders, and selection process, Where * means the always d-connected node.

F.2 THEOREM 4.1

Proof. Causal process: The conditional independence (CI) pattern of the causal process is illustrated in Figure 10, where it demonstrates that the structure $I_X \rightarrow X \rightarrow Y$ forms a chain, and $X \rightarrow Y \leftarrow I_Y$ represents a v-structure. If other d-separated paths exist between X and Y, the causal process can

still be identified by blocking these paths, which can be achieved by conditioning the vertices on the paths. However, cases involving DAG-inducing paths, such as those shown in Figure 11 (b), result in d-connected paths between X and Y , which is the same as the causal process in the CI patterns but is different in structures. Moreover, the structures shown in Figure 11 (a) break the marginal independence of v-structure $I_X \rightarrow X \leftarrow L \rightarrow Y$, working like a causal process as well, leading to partial identification of the causal process.

Latent confounders: The unique structure involving latent confounders is represented by the collider configuration $I_X \rightarrow X \leftarrow L \rightarrow Y \leftarrow I_Y$. If there are d-separated paths between X and Y , the latent confounders can be identified, as the CI pattern remains unaffected when these d-separated paths are blocked. However, cases with DAG-inducing paths, such as the scenario depicted in Figure 11 (d), cannot be identified. This is because the d-connected paths between X and Y mimic the same unique structures associated with latent confounders. However, latent confounders must exist within the d-connected paths, leading to partial identifiability of these confounders.

Selection process: The unique structure of the selection process, characterized by the paths $I_X \rightarrow X \rightarrow S$ and $I_Y \rightarrow Y \rightarrow S$, leads to distinguishable CI patterns, as illustrated in Figure 10. Similarly, cases involving d-separated paths can be identified. However, in scenarios with DAG-inducing paths, such as the one shown in Figure 11 (c), the d-connected paths between X and Y exhibit the same structures, i.e., $I_X \rightarrow X \rightarrow$ and $I_Y \rightarrow Y \rightarrow$. Furthermore, the d-connected property in these cases is identical to that of the selection process, leading to the partial identifiability of the selection process. Consequently, the selection process is only partially identified.

G EXPERIMENTAL RESULTS ON SYNTHETIC DATASET

G.1 GISL V.S. BASELINES WHEN THERE IS NO SELECTION BIAS

The experimental results of GISL and baselines on the data without selection bias are shown in Figure 14. This shows the superiority of utilizing interventional data to recover causal relationships. Compared with canonical baselines, which infer the causal direction based on v-structures, the changes in distribution engendered by intervention provide more information in identifying the causal structure.

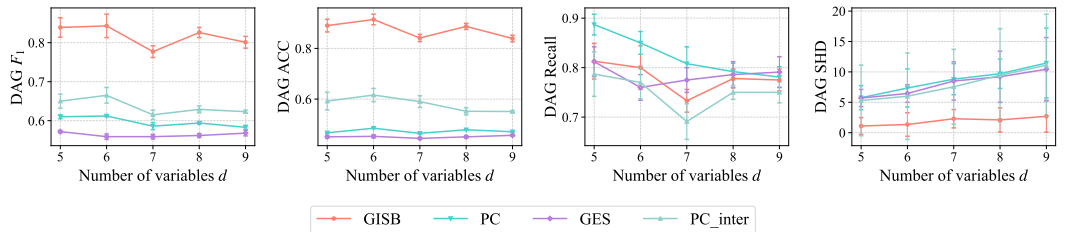


Figure 14: Experimental results of GISB and baselines on synthetic dataset without selection bias.

G.2 GISL V.S. COMPUTATIONAL METHODS UNDER SELECTION BIAS

We rethink the gene regulatory network inference from a causal view and focus on identifying the causal process, latent confounders, and selection process. The setting and output of GISB differ from those of computational methods, which are unable to address the dependencies caused by latent confounders and selection bias. The experimental results of GISB and computational methods on synthetic data are provided for comparison as shown in 2. From the table, it is evident that computational methods fail to identify causal relations in the presence of selection bias. This failure occurs because the selection process affects not only the directly targeted variables but also those connected through the same causal pathways. For example, (C) in Figure 11, if perturbing Y , the distribution of both Z and X changes. Even without gene perturbation data, computational methods that rely solely on dependence (correlation or co-occurrence) consider these variables as dependent. Consequently, their output often results in a fully connected graph.

Table 2: Experimental results of GISB and computational baselines on synthetic data

Methods	Acc	Recall	F1	SHD
GISB	94.7±0.01	95.1±0.01	94.9±0.01	1.0±0.54
PIDC Chan et al. (2017)	21.6±0	95.2±0	35.1±0.03	39.4±62.6
PPCOR Kim (2015)	17.4±0	100.0±0	29.7±0	49±17.6

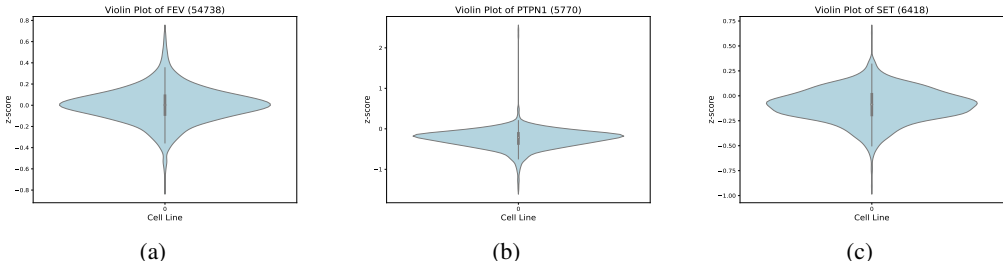


Figure 15: The distribution of z-scores for the genes FEV, PTPN1, and SET across all cell lines highlights the variation in sample size.

H EXPERIMENTAL SETTING OF REAL-WORLD DATASET

Data availability With the advent of next-generation sequencing (NGS) techniques, such as single-cell RNA-sequencing (scRNA-seq), the availability of single-cell data enables a deeper analysis of gene expression in biological systems and complex tissues, offering an unprecedented resolution at the level of individual cells (Saliba et al., 2014). Moreover, thanks to the advancement and maturation of gene sequencing and perturbation tools, including CRISPR-Cas9 (Doudna & Charpentier, 2014), CRISPRi (Larson et al., 2013), and CRISPRa (Cheng et al., 2013), genes are transformed into viable subjects for causal discovery by providing high-quality single-gene observational and perturbation (interventional) data through the systematic technique Perturb-seq (Adamson et al., 2016b; Thomas M. et al., 2019; Dixit et al., 2016).

Evaluation In real-world datasets, the regulatory relationships are evaluated based on Enrichr. However, not all perturbed genes are reported in Enrichr, as some genes cannot be perturbed or processed by biological tools like ChIP-Seq. To evaluate the selection process, a z-score is used to verify its existence. The z-score represents the ratio of the growth rate between perturbed genes and normal genes. Changes in growth rates indicate variations in sample size, which align with the characteristics of the selection process. Thus, the z-score serves as an evaluation tool. Distributions of the z-scores for the reported genes are shown in Figure 15. From the figure, we observe that these genes exhibit differences in growth rates between the perturbed and normal cells, indicating the presence of a selection process. In some cell lines, the growth rate does not change, suggesting that the gene is not under selection in those cells. This observation is consistent with our explanation regarding differential gene expression.

H.1 EXPERIMENTAL RESULTS ON OTHER DATASETS

We conduct experiments on three representative datasets of single-cell gene expression in the real world to verify the effectiveness of our proposed method, including data from K562 cells (Dixit et al., 2016; Adamson et al., 2016a) and Human Lung Epithelial Cells (HLEC) (Thomas M. et al., 2019). Firstly, the skeleton is discovered among 5012 genes. Then, the structure of the perturbed genes is identified. The experimental result on the Dixit dataset is shown in Figure 16. For example, edges RACGAP1 → GABPA, RACGAP1 → ELF1, E2F4 → IRF1, ELF1 → ELK1, GABPA → NR2C2, AURKA → E2F4, YY1 → GABPA etc. are verified as correct by Enrichr, where the ChEA 2022 (Keenan et al., 2019) and TF-gene enrichment (Chen et al., 2013) are mainly considered. We consider them to be more reliable because ChIP-Seq, used in ChEA, directly detects the binding sites between

transcription factors and genes. Additionally, TF-gene enrichment identifies robust pairs supported by enrichment analysis. Moreover, the selection bias is supported by the high z-scores observed for the genes such as *RACGAP1* (-0.903), *E2F4* (-0.158), *GABPA* (-0.543) and *NR2C2* (-0.127), respectively. Experimental results indicate that almost all directed regulatory relationships discovered by GISL are correct, while undirected edges remain undetermined. This is because undirected edges suggest the presence of both selection bias and latent confounders, making the causal process unidentifiable. This is because, with selection bias and latent confounders, the CI pattern becomes fully dependent, which obscures the unique characteristics of causal processes in the CI pattern. The experimental results of PPOCR are shown in Figure 17. The results show that our proposed GISL demonstrates greater accuracy and reliability in matching the results of biological experiments. In addition, the experimental results of GISL on the Norman and Adamson datasets are shown in Figure 18 and Figure 19.

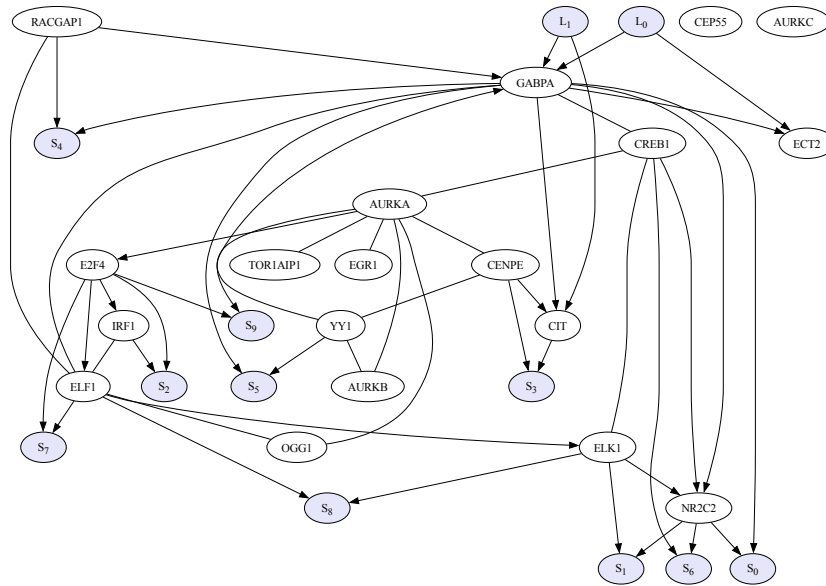


Figure 16: Experimental result of GISL on the Dixit dataset.

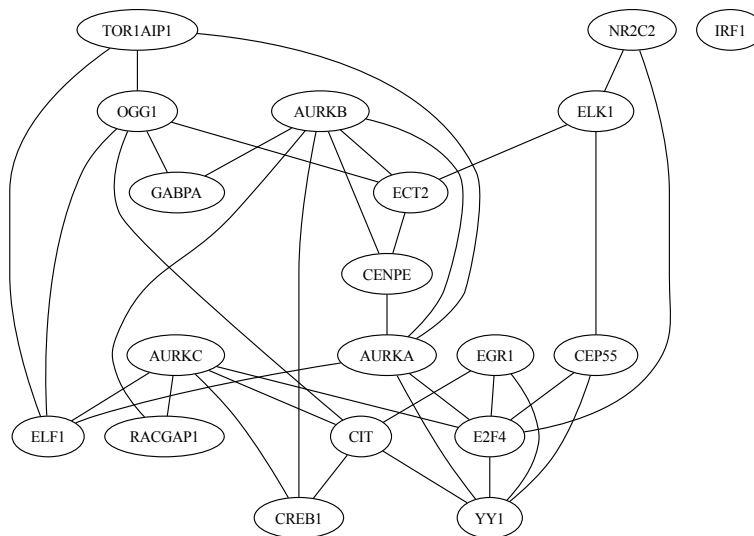


Figure 17: Experimental result of PPCOR on the Dixit dataset.

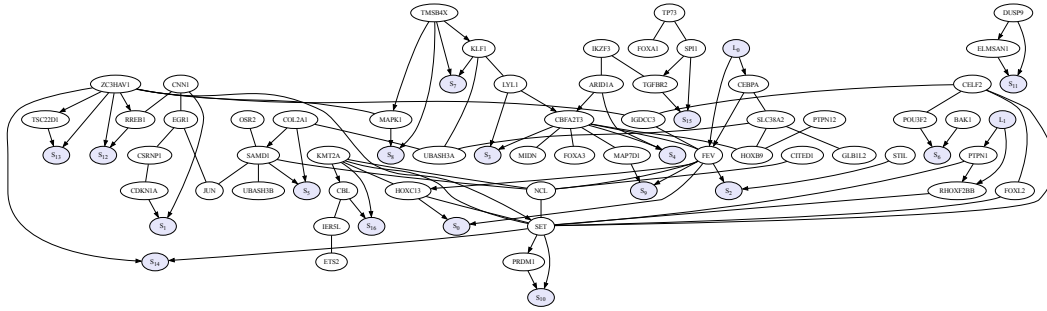


Figure 18: Experimental result of GISL on the Norman dataset.

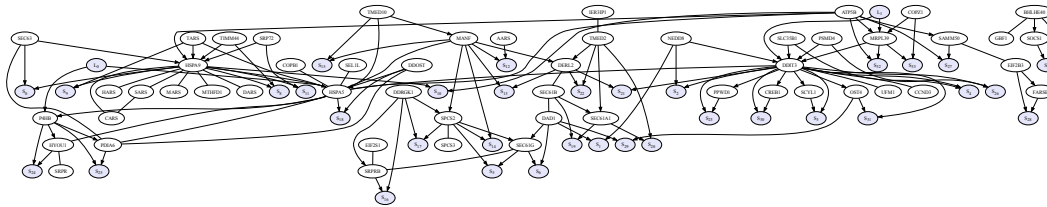


Figure 19: Experimental result of GISL on the Adamson dataset.

I DISCUSSION

Discussion and Limitations. In cells, we argue that the different intracellular environments, acting as selection mechanisms, restrict the expression of genes. When the environment remains, a selection mechanism is always present. Genes stay in cells with the remaining environment, showing the reasonability of our setting. However, at the algorithmic level, if selection does not occur consistently, whether the intervention occurs before or after the selection process will lead to different phenomena. A toy example is designed to introduce this as shown in Figure 20. This interesting discussion is a kind reminder to readers when they apply this algorithm to some specific data, such as patients in hospitals. When they recovered, they were still the sample in the dataset. At this time, the selection mechanism disappears. Some limitations are listed that are willing to be improved in the future. In our setting, we assume that the gene regulatory network is a DAG dealing with acyclic relations. The selection process may also work on latent confounders. We focus on the selection process determined by the measured genes. Moreover, we focus on the soundness and efficacy of our algorithm and do not pay much attention to the efficiency of the CI test.

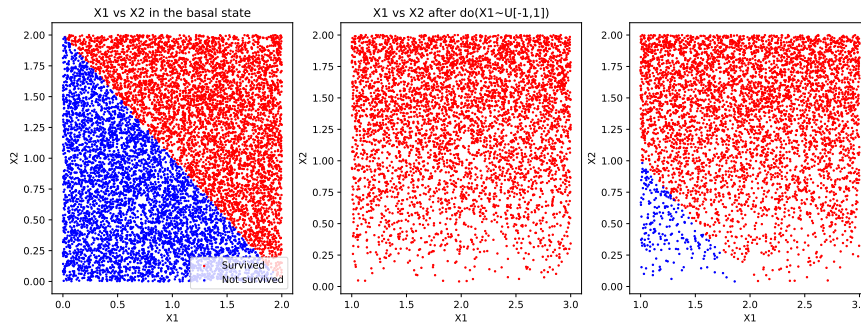


Figure 20: Consistent selection vs. one-time selection.

From Figure 20, we can see that in the figure on the left, $X_1 \perp\!\!\!\perp X_2$. When intervention is done after selection, and the selection does not work anymore, this results in the scatter plot of the middle one. The distribution of $\mathbb{P}(Y|X)$ changes. The last one shows that selection remains. It looks like $\mathbb{P}(Y|X)$ changes from the scatter plot. However, the CI test pattern keeps, that is, $Y \not\perp\!\!\!\perp I_X|S$ and

$Y \perp\!\!\!\perp I_X|X, S$, this is because the increased value range of X is only related to the intervention operation ($I_X = 1$).

Algorithm 4 Concrete procedure of GISL

Input: observational data D_o , single gene perturbation data D_p for perturbed genes with D_{pi} for gene i .

Output: PAG $\mathcal{G} = (\mathcal{V}, \mathcal{E})$, latent pairs \mathcal{L} , selection pairs \mathcal{S} .

Step 1:

Initialize $\mathcal{G} = (\mathcal{V}, \mathcal{E})$ as fully-connected graph.

correct-set = []

condition-set = []

Step 2:

for any pair of genes (x, y) **in** \mathcal{V} **do**

if $x \perp\!\!\!\perp y$ | any subset of $\mathcal{V} - \{x, y\}$ on D_o **then**

 remove the edge between x and y from \mathcal{E} , update \mathcal{G} .

end if

end for

Step 3:

Introduce surrogate variable (perturbation indicator) $I = 0$ for D_o and $I = 1$ for D_p .

for edge between genes (x, y) **in** \mathcal{E} **do**

 Construct D_x by concatenating D_o with $I_X = 0$ and D_{px} with $I_X = 1$. Similarly, construct D_y .

if $x \perp\!\!\!\perp I_Y|s$; $x \not\perp\!\!\!\perp I_Y|y, s$; on D_y , $y \not\perp\!\!\!\perp I_X|s$; $y \perp\!\!\!\perp I_X|x, s$ on D_x **then**

x cause y , update \mathcal{G} .

else if $x \not\perp\!\!\!\perp I_Y|s$; $x \perp\!\!\!\perp I_Y|y, s$; on D_y , $y \perp\!\!\!\perp I_X|s$; $y \not\perp\!\!\!\perp I_X|x, s$ on D_x **then**

y cause x , update \mathcal{G} .

else if $x \not\perp\!\!\!\perp I_Y|s$; $x \perp\!\!\!\perp I_Y|y, s$; on D_y , $y \not\perp\!\!\!\perp I_X|s$; $y \perp\!\!\!\perp I_X|x, s$ on D_x **then**

x and y under selection without cause, update \mathcal{S} with (x, y) .

else if $x \not\perp\!\!\!\perp I_Y|s$; $x \not\perp\!\!\!\perp I_Y|y, s$; on D_y , $y \not\perp\!\!\!\perp I_X|s$; $y \perp\!\!\!\perp I_X|x, s$ on D_x **then**

x cause y under selection bias, update \mathcal{S} with (x, y) , correct-set add (x, y) , condition-set add ('S-C').

else if $x \not\perp\!\!\!\perp I_Y|s$; $x \perp\!\!\!\perp I_Y|y, s$; on D_y , $y \not\perp\!\!\!\perp I_X|s$; $y \not\perp\!\!\!\perp I_X|x, s$ on D_x **then**

y cause x under selection bias, update \mathcal{S} with (x, y) , correct-set add (y, x) , condition-set add ('S-C').

else if $x \perp\!\!\!\perp I_Y|s$; $x \not\perp\!\!\!\perp I_Y|y, s$; on D_y , $y \not\perp\!\!\!\perp I_X|s$; $y \not\perp\!\!\!\perp I_X|x, s$ on D_x **then**

x cause y under latent confounder, update \mathcal{L} with (x, y) , correct-set add (x, y) , condition-set add ('S-L').

else if $x \not\perp\!\!\!\perp I_Y|s$; $x \not\perp\!\!\!\perp I_Y|y, s$; on D_y , $y \perp\!\!\!\perp I_X|s$; $y \not\perp\!\!\!\perp I_X|x, s$ on D_x **then**

y cause x under latent confounder, update \mathcal{L} with (x, y) , correct-set add (y, x) , condition-set add ('S-L').

else if $x \perp\!\!\!\perp I_Y|s$; $x \not\perp\!\!\!\perp I_Y|y, s$; on D_y , $y \perp\!\!\!\perp I_X|s$; $y \not\perp\!\!\!\perp I_X|x, s$ on D_x **then**

x and y under latent confounder without cause, update \mathcal{L} with (x, y) .

else

 correct-set add (y, x) , condition-set add ('C-D'). correct-set add (x, y) , condition-set add ('C-D').

end if

end for

Step 4:

```

for index pair in enumerate correct-set do
   $x, y = \text{pair}[0], \text{pair}[1]$ 
  for all subsets  $s_a$  of nodes on the paths from  $x$  to  $y$  on the path from  $x$  to  $y$  do
    Given subset  $s_a$ 
    if condition-set[index] is 'S-C' then
      if  $x \not\perp\!\!\!\perp I_Y|s; x \not\perp\!\!\!\perp I_Y|y, s; \text{ on } D_y, y \not\perp\!\!\!\perp I_X|s; y \not\perp\!\!\!\perp I_X|x, s \text{ on } D_x$  then
        continue
      else if  $x \not\perp\!\!\!\perp I_Y|s; x \not\perp\!\!\!\perp I_Y|y, s; \text{ on } D_y, y \not\perp\!\!\!\perp I_X|s; y \perp\!\!\!\perp I_X|x, s \text{ on } D_x$  then
        continue
      else if  $x \perp\!\!\!\perp I_Y|s; x \not\perp\!\!\!\perp I_Y|y, s; \text{ on } D_y, y \not\perp\!\!\!\perp I_X|s; y \perp\!\!\!\perp I_X|x, s \text{ on } D_x$  then
         $x$  cause  $y$ , update  $\mathcal{G}$ , continue
      else
        remove edge between  $x$  and  $y$ , update  $\mathcal{G}$ 
        break
      end if
    else if condition-set[index] is 'S-L' then
      if  $x \not\perp\!\!\!\perp I_Y|s; x \not\perp\!\!\!\perp I_Y|y, s; \text{ on } D_y, y \not\perp\!\!\!\perp I_X|s; y \not\perp\!\!\!\perp I_X|x, s \text{ on } D_x$  then
        continue
      else if  $x \perp\!\!\!\perp I_Y|s; x \not\perp\!\!\!\perp I_Y|y, s; \text{ on } D_y, y \not\perp\!\!\!\perp I_X|s; y \not\perp\!\!\!\perp I_X|x, s \text{ on } D_x$  then
        continue
      else if  $x \perp\!\!\!\perp I_Y|s; x \not\perp\!\!\!\perp I_Y|y, s; \text{ on } D_y, y \not\perp\!\!\!\perp I_X|s; y \perp\!\!\!\perp I_X|x, s \text{ on } D_x$  then
         $x$  cause  $y$ , update  $\mathcal{G}$ , continue
      else
        remove edge between  $x$  and  $y$ , update  $\mathcal{G}$ 
        break
      end if
    else if condition-set[index] is 'C-D' then
      if  $x \perp\!\!\!\perp I_Y|s; x \not\perp\!\!\!\perp I_Y|y, s; \text{ on } D_y, y \not\perp\!\!\!\perp I_X|s; y \perp\!\!\!\perp I_X|x, s \text{ on } D_x$  then
         $x$  cause  $y$ , update  $\mathcal{G}$ .
      else if  $x \not\perp\!\!\!\perp I_Y|s; x \perp\!\!\!\perp I_Y|y, s; \text{ on } D_y, y \not\perp\!\!\!\perp I_X|s; y \perp\!\!\!\perp I_X|x, s \text{ on } D_x$  then
         $x$  and  $y$  under selection without cause, update  $\mathcal{S}$  with  $(x, y)$ .
      else if  $x \not\perp\!\!\!\perp I_Y|s; x \not\perp\!\!\!\perp I_Y|y, s; \text{ on } D_y, y \not\perp\!\!\!\perp I_X|s; y \perp\!\!\!\perp I_X|x, s \text{ on } D_x$  then
         $x$  cause  $y$  under selection bias, update  $\mathcal{S}$  with  $(x, y)$ .
      else if  $x \perp\!\!\!\perp I_Y|s; x \not\perp\!\!\!\perp I_Y|y, s; \text{ on } D_y, y \not\perp\!\!\!\perp I_X|s; y \not\perp\!\!\!\perp I_X|x, s \text{ on } D_x$  then
         $x$  cause  $y$  under latent confounder, update  $\mathcal{L}$  with  $(x, y)$ .
      else if  $x \perp\!\!\!\perp I_Y|s; x \not\perp\!\!\!\perp I_Y|y, s; \text{ on } D_y, y \perp\!\!\!\perp I_X|s; y \not\perp\!\!\!\perp I_X|x, s \text{ on } D_x$  then
         $x$  and  $y$  under latent confounder without cause, update  $\mathcal{L}$  with  $(x, y)$ .
      end if
    end if
  end for
end for
end for
return PAG  $\mathcal{G} = (\mathcal{V}, \mathcal{E})$ , selection pairs  $\mathcal{S}$ , latent confounders  $\mathcal{L}$ .

```
